

Field-free molecular orientation with terahertz few-cycle pulses

Chuan-Cun Shu,^{a)} Kai-Jun Yuan, Wen-Hui Hu, and Shu-Lin Cong^{b)}
Department of Physics, Dalian University of Technology, Dalian 116024, China

(Received 26 January 2010; accepted 10 June 2010; published online 28 June 2010)

We demonstrate theoretically an efficient field-free orientation in LiH and LiCl driven by available terahertz few-cycle pulses (TFCPs). Exact results by numerically solving the time-dependent Schrödinger equation including the vibrational and rotational degrees of freedom are compared to the rigid-rotor approximation (RRA) as well as to the impulsive approximation (IA), and the effect of rotational-vibrational coupling on the both RRA and IA is examined in detail. We find that the current available TFCPs may overcome the technical limitation of terahertz half-cycle pulse for enhancing the field-free molecular orientation. © 2010 American Institute of Physics.
 [doi:10.1063/1.3458913]

I. INTRODUCTION

For a large range of experiments in chemistry and physics, highly aligned or oriented molecules in gas-phase are very important, and molecular alignment or orientation driven by laser pulses is an active field of research, which has attracted much attention in control of chemical reactions, nanoscale design, high harmonics generation, and quantum-information processing.^{1–8} Many of the introductory and methodology details were summarized in a review article on nonadiabatic alignment and orientation.⁹ Recent study has demonstrated that the multiphoton ionization (MPI) depends strongly on molecular orientation, explaining suppression and enhancement of MPI at corresponding orientation.¹⁰ In our recent research, the field-free molecular orientation is proposed to determine the carrier-envelope phase of few-cycle pulses.¹¹

Laser-controlled molecular orientation, which refers to the molecular axis pointing to a particular direction, continues to be a challenge to both experiment and theory. Different methods have been proposed for orienting molecules with static electric fields or laser fields, or both,^{12–19} and a few techniques have been experimentally demonstrated.^{20–23} Techniques for laser orientation of gas-phase molecules can be divided into two regimes, adiabatic and impulsive, depending on the relative duration of the laser pulse and the average time of rotation of the molecules in the ensemble. In the adiabatic regime, strong nonresonant pulses with a temporal width longer than the rotational period of the molecule can generate efficiently molecular orientation only in the presence of the laser fields. The most recent experimental study has reported an alternative approach to achieve all-optical orientation of the molecules with an intense nonresonant two-color laser field in the adiabatic regime.²⁴ Since the strong external field accompanying orientation may undesirably modify the physical or chemical property of the gas molecules, the field-free orientation is widely desired in most applications. For an impulsive orientation, two groups have

demonstrated laser-field-free transient molecular orientation in the presence of a dc electric field.^{21,23} Recently, Kling and co-workers²⁵ experimentally presented an important approach to generate a complete field-free orientation of CO molecules using two-color strong laser fields ($\sim 10^{14}$ W/cm²), which was extensively studied in theory.^{26,15,27} The strong laser fields leading to ionization or the presence of a dc electric field might limit the application of these techniques. A recent study suggested that the field-free molecular orientation can be controlled by sequential three-photon Raman excitation with time-delayed dual-color ultrashort laser pulses.²⁸

To generate an impulsive field-free molecular orientation, many theoretical schemes have been proposed by using terahertz half-cycle pulse (HCP),^{29,30} which can exert a rapid “kick” to drive the molecular axis toward the laser field direction. However, it has not been confirmed experimentally so far. The experimental difficulties of all these control scenarios lie in that the generation and application of electromagnetic radiation in frequency range of [0.1,10] THz (1 THz=33 cm⁻¹) are still far less developed than that in other frequency ranges, and most terahertz generation techniques provide quite low terahertz field strength. In our recent work,³¹ a promising strategy with the use of experimentally available terahertz few-cycle pulses³² (TFCPs) was proposed to break this predicament. Here, we study the field-free molecular orientation with TFCPs in two different molecules. Of particular interest in the present study is how to understand the field-free molecular orientation driven by TFCPs using different levels of approximation. We find that the application of terahertz few-cycle pulses can also enhance the field-free molecular orientation, suggesting a new approach for overcoming the technical limitation of terahertz HCPs.

The remainder of this paper is organized as follows. In Sec. II, we present theoretical treatments based on three levels of approximations: the exact solution of the time-dependent Schrödinger equation (TDSE) including the rotational and vibrational degrees of freedom, the rigid-rotor approximation (RRA), and the impulsive approximation

^{a)}Electronic mail: scchenmo@126.com.

^{b)}Electronic mail: shlcong@dlut.edu.cn.

(IA). The numerical results and discussions are presented in Sec. III. Finally, some conclusions are given in Sec. IV.

II. THEORETICAL METHOD

We consider a polar diatomic molecule initially in its electronic ground state. Since the TFCPs with moderate intensities are used in the present study, the dipole coupling is dominant and polarizability interaction is close to zero.³¹ Within the Born–Oppenheimer approximation,^{33,34} the time evolution of the molecule interacting with a linearly polarized fields is governed by TDSE,

$$i\hbar \frac{\partial}{\partial t} \Psi(t) = \hat{H}(t) \Psi(t). \quad (1)$$

The total Hamiltonian is $\hat{H}(t) = [\hat{H}_0 + \hat{H}_I(t)]$, where \hat{H}_0 is the field-free Hamiltonian, and \hat{H}_I represents the interaction between the molecule and terahertz radiation via the dipole moment.

A. Full rovibrational description

By including the vibrational and rotational degrees of freedom, the field-free molecular Hamiltonian \hat{H}_0 can be expressed as

$$\hat{H}_0 = -\frac{\hbar^2}{2mR^2} \frac{\partial}{\partial R} \left(R^2 \frac{\partial}{\partial R} \right) + \frac{\hbar^2 \hat{J}^2}{2mR^2} + \hat{V}(R), \quad (2)$$

where m is the reduced mass, R is the internuclear separation, $\hat{V}(R)$ is the internuclear potential, and \hat{J} is the angular momentum operator. The details of the rovibrational Hamiltonian can be found in Refs. 35 and 36.

For a linear molecule having a permanent dipole moment $\mu(R)$, the field-molecule interaction Hamiltonian \hat{H}_I can be written as

$$\hat{H}_I(t) = -\mu(R)\epsilon(t)\cos\theta, \quad (3)$$

where θ is the angle between the molecular axis and the polarization direction of TFCPs, and the total electric field is described by

$$\epsilon(t) = \sum_{k=1,2} f_k(t) \cos[\omega(t - \tau_k) + \phi], \quad (4)$$

with the Gaussian temporal profile

$$f_k(t) = E_k \exp\left[-\frac{4 \ln 2}{t_p^2} (t - \tau_k)^2\right], \quad (5)$$

where E_k and τ_k are the field amplitude and center time of the k th pulse, respectively. ω is the center frequency, ϕ is the carrier-envelope phase (CEP) of the pulse, and t_p is the full-width at half-maximum (FWHM). The FWHM t_p should be tuned to match the period of the pulse $\tau = 2\pi/\omega$, i.e., $t_p = n\tau$ ($n=1, 2, 3, \dots$) for a FCP and $t_p = \tau/2$ for a single HCP.

In the linearly polarized TFCPs, the magnetic quantum number M of a molecule is conserved. The wave function can be expressed in an expansion as²⁹

$$\Psi_M(R, \theta, \varphi, t) = \sum_J \chi_J(R, t) Y_{J,M}(\theta, \varphi). \quad (6)$$

Assuming that the molecule initially was in an eigenstate of the Hamiltonian, a measure of the degree of orientation is given by the dynamical expectation value of $\cos\theta$,

$$\langle \cos\theta \rangle(t) = \langle \Psi_M(R, \theta, \varphi, t) | \cos\theta | \Psi_M(R, \theta, \varphi, t) \rangle. \quad (7)$$

B. Rigid-rotor approximation

In the case of no vibrational excitation, the instantaneous Hamiltonian $\hat{H}(t)$ within the RRA can be written as

$$\hat{H}(t) = B_e \hat{J}^2 - \mu(R_e) \epsilon(t) \cos\theta, \quad (8)$$

where $B_e = \hbar^2 / (2mR_e^2)$ and $\mu(R_e)$ are the rotational constant and the permanent dipole moment at equilibrium nuclear distance R_e , respectively. The time-dependent wave function $|\Psi_M(t)\rangle$ can be represented by the expansion

$$|\Psi_M(t)\rangle = \sum_J C_{JM}(t) |JM\rangle e^{-iE_{JM}t/\hbar}, \quad (9)$$

where E_{JM} is the eigenenergy of rotational state $|JM\rangle$.

The degree of orientation can thus be numerically evaluated. Note that as the TFCPs are turned on, only the matrix elements $U_{JM, J\pm 1M} = \langle JM | \cos\theta | J\pm 1M \rangle$ are not equal to zero according the property of spherical harmonic functions. Thus, the degree of orientation can be expressed explicitly as

$$\langle \cos\theta \rangle(t) = 2 \sum_{J=0} |C_{JM}(t)| |C_{J+1M}(t)| U_{JM, J+1M} \times \cos(\Delta\omega_J t - \psi_{J+1J}), \quad (10)$$

where

$$\Delta\omega_J = (E_{J+1} - E_J)/\hbar = 2B_e(J+1)/\hbar \quad (11)$$

and

$$\psi_{J+1J} = \arg(C_{J+1M}) - \arg(C_{JM}). \quad (12)$$

Since $\arg(C_{JM})$ depends on the CEP of TFCP, the relative phase ψ_{J+1J} can be controlled by ϕ . Therefore, a simple dependence of the degree of orientation on the CEP of TFCP can be observed,³¹ suggesting that CEP is an important parameter for controlling molecular orientation.

C. Impulsive approximation

If the rotational period of a molecule is much longer than the duration of TFCPs, the interaction of the molecule with the TFCPs can be understood as an instantaneous momentum transfer or impulsive kick.^{30,37,38} A few-cycle pulse consists of a series of half-cycle, in which the sign of the electric field is reversed with each half-cycle. Within the IA, $\epsilon(t)$ consisting of N half-cycles can be described by a series of N consecutive kicks,³¹ and therefore the Hamiltonian of the kicked rotor is given by

TABLE I. Molecular parameters.

Molecule	B_e (cm^{-1})	$\mu(R_e)$ (D)	T_{rot} (ps)	ω_e (cm^{-1})
LiH	7.51	5.83	2.221	1406
LiCl	0.7064	7.27	23.614	644.09

$$\hat{H}(t) = B_e \hat{J}^2 - \mu(R_e) \cos \theta \sum_{i=1}^N \Delta p_i \delta(t - t_i), \quad (13)$$

where Δp_i is the area enclosed by the i th half-cycle with center time t_i . Physically, the impulse imparted to the molecule by the i th kick is characterized by kick strength $P_i = \mu(R_e) \Delta p_i / \hbar$. As a result of the i th kick being applied to the rotor at $t=t_i$, the system dynamics can be described by^{39,40}

$$\Psi(t_i + 0) = e^{-(i/\hbar)B_e(t_i+0)} \hat{J}^2 e^{iP_i \cos \theta} \Psi(t_i - 0), \quad (14)$$

with

$$e^{iP_i \cos \theta} = \sum_{J=0}^{\infty} (2J+1) i^J j_J(P_i) P_J(\cos \theta), \quad (15)$$

where $P_J(\cos \theta)$ is the Legendre polynomial and $j_J(P_i)$ is the spherical Bessel function of the J th order. Therefore, laser pulse during every half-cycle can impart a kick on the molecule and transfer its angular momentum to the molecule. The consequence is to generate an oriented wave packet involving a limited number of rotational states.

III. NUMERICAL RESULTS AND DISCUSSION

To demonstrate the efficiency of the field-free orientation driven by TFCPs, we present a complete analysis both in LiH and in LiCl in the electronic ground state $X^1\Sigma^+$ starting from an initial isotropic angular distribution ($J=M=0$) at zero rotational temperature $T=0$ K. The details of the numerical calculation of the time-dependent Schrödinger equation can be found in our previous paper.⁴¹ The accurate molecular parameters for LiH and LiCl are available from Refs. 42 and 43. The relevant constants for the two molecules are listed in Table I. The most recent terahertz technology has made it possible to generate the TFCPs with FWHM of 100 fs, peak electric field amplitudes of 1.08×10^8 V/cm ($\sim 1.55 \times 10^{13}$ W/cm²), and center frequencies continuously tunable from 10 to 72 THz.³² All pulse parameters used in our calculation are available based on the present terahertz technology.

A. Field-free orientation of LiH

Figure 1(a) depicts the electric field of The TFCPs used for the exact TDSE solution and the RRA (solid line), and the pulse used for the IA by a series of delta function kick (dashed lines). The center frequency is taken to be $\omega = 10$ THz. The peak electric field amplitude of the first laser pulse with center time of $\tau_1=0$ is fixed at $E_1=2.0 \times 10^7$ V/cm ($\sim 5.31 \times 10^{11}$ W/cm²), and $E_2=1.6 \times 10^7$ V/cm ($\sim 3.4 \times 10^{11}$ W/cm²) for the second laser pulse with $\tau_2=52$ fs. The amplitude spectrum, obtained by a

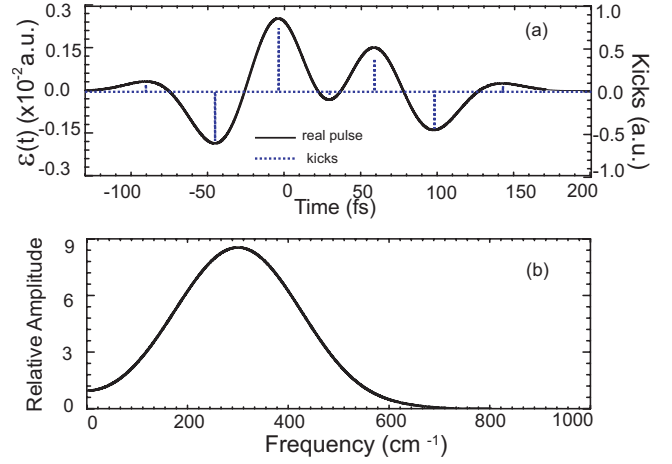


FIG. 1. (a) Electric field (solid line) used for the exact TDSE and RRA calculations, and kicked field (dashed lines) consisting of seven consecutive kicks used for the IA. (b) Fourier transforms of pulse $E_1 \exp[-(4 \ln 2/t_p^2) \times (t - \tau_1)^2] \cos[\omega(t - \tau_1)]$ in frequency domain. $E_1=2.0 \times 10^7$ V/cm ($\sim 5.31 \times 10^{11}$ W/cm²), $E_2=1.6 \times 10^7$ V/cm ($\sim 3.4 \times 10^{11}$ W/cm²), $\tau_1=0$ fs, $\tau_2=52$ fs, $\omega=330$ cm^{-1} , $t_p=100$ fs, and $\phi=0$.

numerical Fourier transform of $E_1 \exp[-(4 \ln 2/t_p^2) \times (t - \tau_1)^2] \cos[\omega(t - \tau_1)]$,⁴⁴ is displayed in Fig. 1(b). Figure 2 shows the $\langle \cos \theta \rangle(t)$ calculated by using the TDSE reported in our previous study,³¹ the RRA and the IA. The rotational revivals of oriented wave packets are present in the present study. Revival structure is an important character of aligned or oriented wave packet. Seideman⁴⁵ demonstrated numerically and analytically the revival structure of spatially aligned wave packets under field-free condition. From Eq. (11), we can find that all the frequencies are equal to integer times of $2B_e/\hbar$, which means that the dephasing and revival in the wave packet will occur at the revival time $\tau_{\text{rev}} = \pi\hbar/B_e$. In Fig. 2, we can observe the evident orientation revivals spaced by the rotational period $T_{\text{rot}} = \pi\hbar/B_e$, which is in good agreement with the theoretical predication.

The agreement of the calculated results between the full solution of TDSE and the RRA is excellent, indicating that there is no effect of the vibrational excitations on the orientation dynamics. From Fig. 1(b), we can find that the frequency of terahertz pulse is far from the fundamental vibrational frequency ($\omega_e=1406$ cm^{-1}) of LiH. The field will exert an unabiding force on the permanent dipole moment of the molecule, and then the molecule will exchange angular momentum with the external field by rotational excitations. Moreover, since the molecule is initially populated in the ν

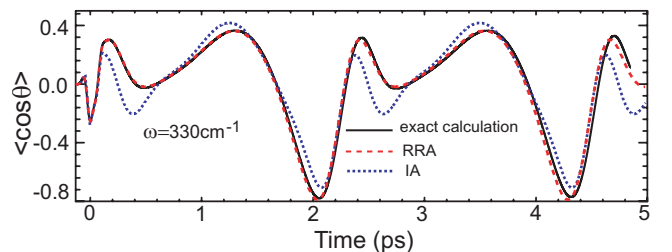


FIG. 2. The evolution of the degree of orientation $\langle \cos \theta \rangle(t)$ for LiH using the three levels of approximations, where the rotational temperature is $T=0$ K.

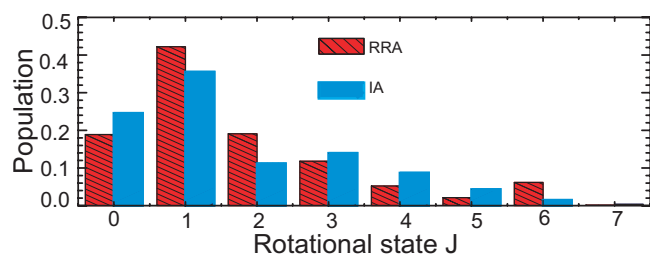


FIG. 3. The final rotational populations calculated by the RRA and the IA for LiH.

=0 vibrational state, the effect of the vibrational motion is negligible. Thus, the purely nonadiabatic rotational excitation can be well described by the RRA.

The result calculated by using the IA cannot reproduce quantitatively the exact result, but it is in qualitative agreement with the exact result. The difference results from the effect of temporal shape and rise time on the orientation process because the temporal width of half-cycle is not negligible with respect to T_{rot} of LiH.³⁰ Figure 3 shows the final rotational populations calculated by using the RRA and the IA. In both cases, the rotational wave packet is created in a wide range from $J=0$ to $J=7$, but there is an evident difference between the RRA and the IA. It is clear from Eq. (10) that since $\langle JM|\cos\theta|J+1M\rangle$ is a series of positive-definite fixed values for different rotational states, the degree of orientation is determined by rotational populations and the relative phase $\psi_{J+1,J}$. Therefore the results of orientation are different, and there is a phase difference for orientation evolution between the RRA and the IA in the field-free situation.

B. Field-free orientation of LiCl

We now discuss the orientation dynamics of LiCl with a longer rotational period, $T_{\text{rot}}=23.614$ ps. Figure 4 shows the time evolution of $\langle\cos\theta\rangle(t)$ as a function of laser frequency ω from 310 to 360 cm^{-1} , where the intensities of electric fields are increased to $E_1=2.5\times 10^7$ V/cm and $E_2=2.0\times 10^7$ V/cm, and other parameters are unchanged. The field-free molecular orientation with an impressive value of $|\langle\cos\theta\rangle_{\text{max}}|=0.81$ can be created, and there exists a regime of $\omega<350$ cm^{-1} in which the maximum orientation $|\langle\cos\theta\rangle_{\text{max}}|$ can exceed the saturation limit of $\langle\cos\theta\rangle=0.75$ obtained by

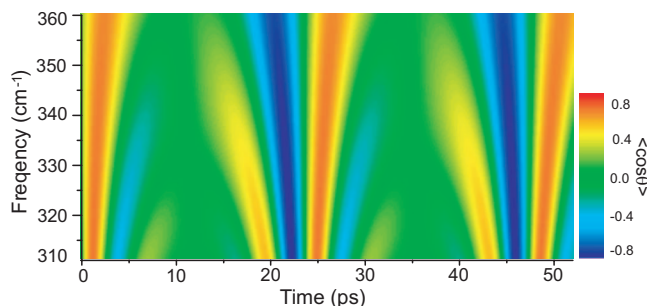


FIG. 4. The evolution of the degree of orientation $\langle\cos\theta\rangle(t)$ for LiCl as a function of laser frequency ω , where the intensity of electric fields are $E_1=2.5\times 10^7$ V/cm and $E_2=2.0\times 10^7$ V/cm, and the other pulse parameters are the same as those in Fig. 1.

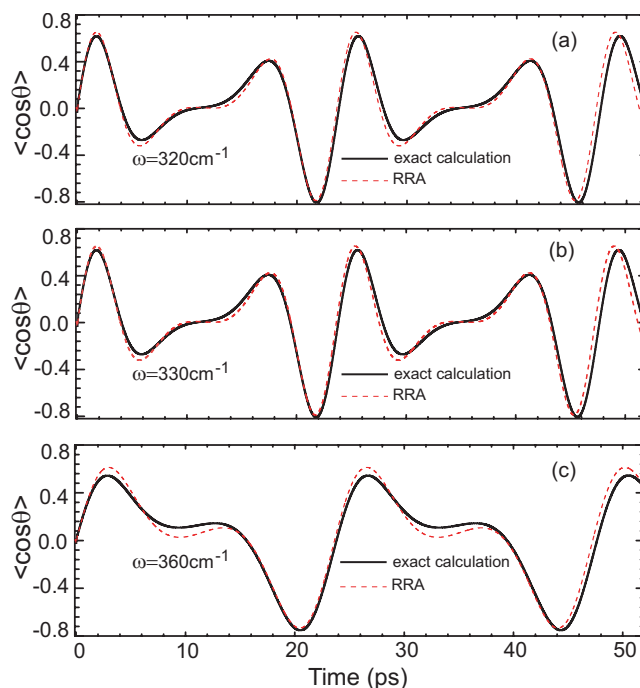


FIG. 5. The evolutions of the degree of orientation $\langle\cos\theta\rangle(t)$ obtained by using the exact TDSE calculation and the RRA for LiCl.

using a single high intensity HCP. Hence, the degree of orientation in the present study is high enough to enable its application. The best orientation is obtained by confining the molecule to a narrow angular distribution of $\Delta\theta$, which corresponds to a broad rotational band of ΔJ according to the uncertainly principle $\Delta J\Delta\theta\geq\hbar/2$.^{17,46} By conversing this principle to the time domain, we can find that better degree of orientation, the shorter the duration of orientation. Contrarily, the lower degree of orientation, the longer the orientation duration. Thus, we can find that orientation duration is prolonged when the degree of orientation decreases in Fig. 4. For application, it is important to reach a sufficient orientation duration, which has also received considerable attention.⁴⁷

To test the validity of the RRA for LiCl, Fig. 5 shows the comparisons of $\langle\cos\theta\rangle(t)$ between the exact TDSE calculation and the RRA calculation at three different frequencies. The resulting dynamics of $\langle\cos\theta\rangle(t)$ is nearly indistinguishable at the lower frequency $\omega=320$ cm^{-1} . There is a slight difference between the two results at the higher frequency, which may result from the rovibrational excitations because the RRA model does not include vibrational modes. For a polar molecule interacting with few-cycle pulse, the two-photon transition can be allowed due to the presence of the permanent dipole moment.^{48,49} Although the laser frequency used in the calculation is far below the fundamental vibrational frequency of LiCl, the strong laser pulses may induce the rovibrational transitions via two-photon process since ac field-permanent dipole interaction (Stark shift)- $\mu(R)\cos\theta\epsilon(t)$ leading to an energy shift can modify the transition frequencies. On the other hand, an important quality of ultrashort laser pulses is their spectral width. From Fig. 1(b), we can find that the pulse frequency used in our calculation is enough to satisfy the two-photon resonance

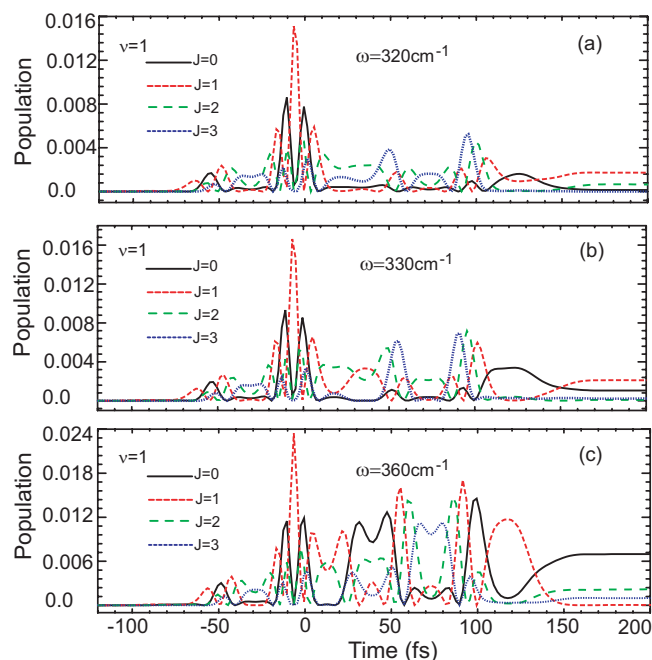


FIG. 6. Time-dependent rotational populations of $J \leq 3$ in the $\nu=1$ vibrational state for LiCl.

condition for rovibrational transitions. Hence, the TFCPs excite nonadiabatically the molecule to a time-dependent superposition of field-free rotational eigenstates belonging in different vibrational manifolds.

To confirm the above analysis, Fig. 6 displays the time-dependent rotational populations of $J \leq 3$ in the $\nu=1$ vibrational state. The results in Fig. 6 clearly show that the rovibrational transitions take place. The initial population is partially transferred to the $\nu=1$ vibrational state with $\Delta J=0$ and ± 2 transitions, and subsequent $\Delta J = \pm 1$ excitations further transfer the population to other rotational states. As a result, the nonadiabatic rovibrational excitations driven by TFCPs lead to the formation of a rotational wave packet in the $\nu=1$ vibrational state. Moreover, since the energy shifts caused by ac Stark shift are dependent on the sign of field of TFCPs, the rapid oscillations of rotational populations can be observed from Fig. 6. It is interesting to note that at the lower frequency, $\omega=320 \text{ cm}^{-1}$, although the laser frequency is in near two-photon resonant with a vibrational frequency of $\omega_e=644.09 \text{ cm}^{-1}$, the rovibrational excitations are hindered. This should be attributed to the effect of the ac Stark shift on rovibrational transitions. At the higher frequencies, however, we can find that the stronger rovibrational excitations, the better orientation, indicating that the rovibrational excitations can enhance the molecular orientation. The effect of the rovibrational excitations on orientation will be further enhanced so that the RRA will fail evidently, if the pulse intensity becomes strong, or the pulse frequency is tuned to resonance well. A completely rovibrational pre-excitation enhancing the field-free molecular orientation has been discussed in our previous papers.^{50,51}

It is worth noticing that if the duration of TFCPs much shorter than the rotational period of the molecule, the laser-molecule interaction gives a rapid kick to move the molecular axis toward the field direction of TFCPs. This condition

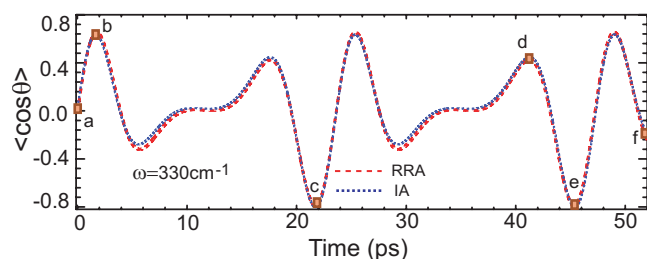


FIG. 7. The evolutions of the degree of orientation $\langle \cos \theta \rangle(t)$ calculated by using the RRA and the IA for LiCl. The letter marks indicate the short instants.

can be well satisfied for LiCl with rotational period $T_{\text{rot}} = 23.614 \text{ ps}$. Figure 7 shows the calculations of $\langle \cos \theta \rangle(t)$ using the RRA and IA at the lower frequency, $\omega = 330 \text{ cm}^{-1}$. The evolution of the degree of orientation using the IA is in good agreement with that using the RRA. The orientation dynamics for LiCl can thus be well understood within the frame of delta-kicked rotor model, in which the orientation dynamics depends mainly on the time-integrated electric field rather than the pulse shape or rise time.³⁰ Actually, the effect of TFCPs is similar to a train of HCPs. Theoretical studies have already shown that a train of HCPs can enhance the degree of orientation.⁵² Therefore, we can take advantage of the available TFCPs to replace the train of HCPs for generating efficient field-free molecular orientation, which might overcome the current technical limitation of terahertz HCPs.

To further gain insight into the feature underlying the IA, Fig. 8 shows the angular distributions of wave packet at six different times. Since the angular momentum of LiCl is not conserved in the presence of the electric field, the TFCPs with a few kicks cause the rotational excitations bringing the molecule from a completely isotropic angular distribution to a more oriented configuration. The angular distribution displays a rich variety of spatial asymmetries with periodic inversion, which indicates that the rotational wave packet freely evolves after the kicks are over. The evolution of field-free molecular orientation depends on the distribution of rotational states. Therefore, by controlling the rotational population one can obtain a desired molecular orientation with sufficient orientation duration,^{17,52,53} and the rotational quantum state might be reconstructed experimentally.^{54–56}

It should be pointed out that the pulse parameters used in the present work are not optimized. The optimized pulse parameters could be employed to obtain more efficient orientation with higher orientation value and longer orientation duration. An experimental realization and its application for the present study are very desirable. For example, having the ability to prepare quantum states with a well-defined orientation of the molecular axis is essential to measure the electric dipole moment in the latest experiment.⁵⁷ An interesting application of the present study is the generation of electric ring currents,^{58,59} which depends on sharp orientation of the molecule with respect to the excitation field. Moreover, York and Milchberg showed that laser-aligned molecules can amplify broadband terahertz radiation, allowing high-energy amplification of few-cycle pulses at terahertz frequencies.⁶⁰

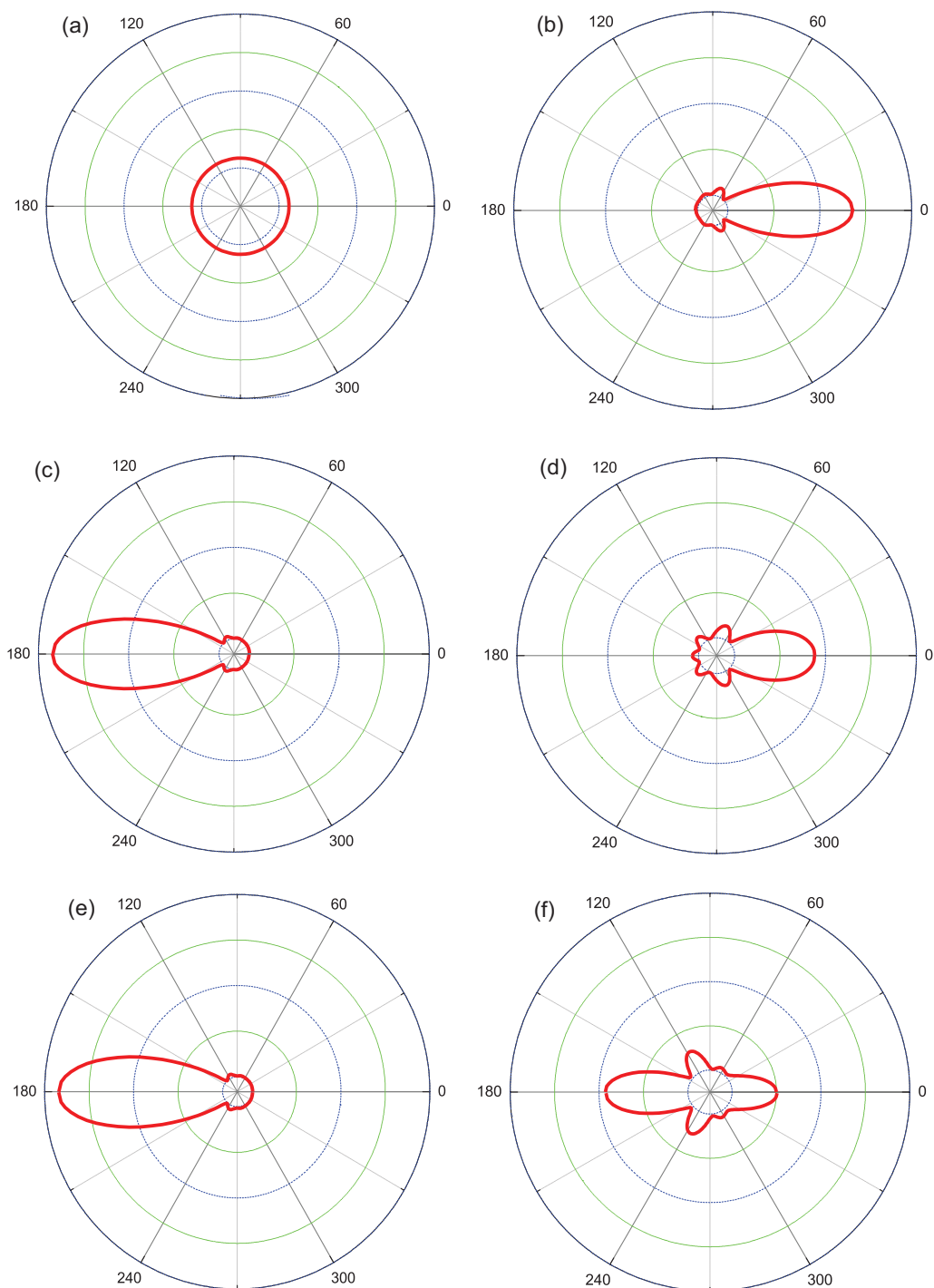


FIG. 8. Polar plots of angular distributions at different times marked in Fig. 7 for LiCl.

A question of particular interest is whether laser-oriented molecules can radiate strong terahertz pulses.

IV. CONCLUSION

We have theoretically investigated the field-free molecular orientation driven by experimentally available TFCPs. The calculations are carried out using three different methods, with LiH and LiCl as the examples. The results of the three methods are compared, and the effect of rotational-vibrational coupling on the both RRA and IA is discussed in detail. The exact TDSE solution can confirm the possibility

of generating stronger orientation with TFCPs. The RRA and IA can give an important insight of orientation dynamics. When the rotational period of a molecule is much longer than TFCPs temporal width, we find that the field-free molecular orientation driven by TFCPs can be well understood by a train of HCPs kicking the rotor, providing a new approach for enhancing the degree of orientation. Moreover, rovibrational pre-excitation enhancing the field-free molecular orientation is also observed in LiCl. We believe that the present work associated with recent advances in TFCPs may promote new applications for understanding and controlling molecular processes.

ACKNOWLEDGMENTS

C.-C.S and K.-J.Y are very grateful to Dr. I. Barth (Berlin) for many fruitful discussions and useful suggestions. C.-C.S acknowledges the Special Fund from the Central Collegiate Basic Scientific Research Bursary. This work was supported by the National Natural Science Foundation of China under Grant Nos. 10974024 and 20633070.

- ¹T. P. Rakitzis, A. J. van den Brom, and M. H. M. Janssen, *Science* **303**, 1852 (2004).
- ²H. Ohmura, N. Saito, and M. Tachiya, *Phys. Rev. Lett.* **96**, 173001 (2006).
- ³M. G. Reuter, M. Sukharev, and T. Seideman, *Phys. Rev. Lett.* **101**, 208303 (2008).
- ⁴H. Hou, S. J. Gulding, C. T. Rettner, A. M. Wodtke, and D. J. Auerbach, *Science* **277**, 80 (1997).
- ⁵E. A. Shapiro, M. Spanner, and M. Y. Ivanov, *Phys. Rev. Lett.* **91**, 237901 (2003).
- ⁶R. Velotta, N. Hay, M. B. Mason, M. Castillejo, and J. P. Marangos, *Phys. Rev. Lett.* **87**, 183901 (2001).
- ⁷T. Kanai, S. Minemoto, and H. Sakai, *Nature (London)* **435**, 470 (2005).
- ⁸R. Torres, N. Kajumba, J. G. Underwood, J. S. Robinson, S. Baker, J. W. G. Tisch, R. de Nalda, W. A. Bryan, R. Velotta, C. Altucci, I. C. E. Turcu, and J. P. Marangos, *Phys. Rev. Lett.* **98**, 203007 (2007).
- ⁹T. Seideman and E. Hamilton, *Adv. At., Mol., Opt. Phys.* **52**, 289 (2005).
- ¹⁰S.-K. Son and S.-I. Chu, *Phys. Rev. A* **80**, 011403 (2009).
- ¹¹C.-C. Shu, K.-J. Yuan, W.-H. Hu, and S.-L. Cong, *Opt. Lett.* **34**, 3190 (2009).
- ¹²L. Cai, J. Marango, and B. Friedrich, *Phys. Rev. Lett.* **86**, 775 (2001).
- ¹³S. Guérin, L. P. Yatsenko, H. R. Jauslin, O. Faucher, and B. Lavorel, *Phys. Rev. Lett.* **88**, 233601 (2002).
- ¹⁴D. V. Zhdanov and V. N. Zadkov, *Phys. Rev. A* **77**, 011401 (2008).
- ¹⁵R. Tehini and D. Sugny, *Phys. Rev. A* **77**, 023407 (2008).
- ¹⁶M. Muramatsu, M. Hita, S. Minemoto, and H. Sakai, *Phys. Rev. A* **79**, 011403 (2009).
- ¹⁷J. Salomon, C. M. Dion, and G. Turinici, *J. Chem. Phys.* **123**, 144310 (2005).
- ¹⁸R. Baumfalk, N. H. Nahler, and U. Buck, *J. Chem. Phys.* **114**, 4755 (2001).
- ¹⁹B. Friedrich, N. H. Nahler, and U. Buck, *J. Mod. Opt.* **50**, 2677 (2003).
- ²⁰H. Sakai, S. Minemoto, H. Nanjo, H. Tanji, and T. Suzuki, *Phys. Rev. Lett.* **90**, 083001 (2003).
- ²¹A. Goban, S. Minemoto, and H. Sakai, *Phys. Rev. Lett.* **101**, 013001 (2008).
- ²²L. Holmegaard, J. H. Nielsen, I. Nevo, H. Stapelfeldt, F. Filsinger, J. Küpper, and G. Meijer, *Phys. Rev. Lett.* **102**, 023001 (2009).
- ²³O. Ghafur, A. Rouzée1, A. Gijsbertsen, W. K. Siu, S. Stolte, and M. J. J. Vrakking, *Nat. Phys.* **5**, 289 (2009).
- ²⁴K. Oda, M. Hita, S. Minemoto, and H. Sakai, *Phys. Rev. Lett.* **104**, 213901 (2010).
- ²⁵S. De, I. Znakovskaya, D. Ray, F. Anis, N. G. Johnson, I. A. Bocharova, M. Magrakvelidze, B. D. Esry, C. L. Cocke, I. V. Litvinyuk, and M. F. Kling, *Phys. Rev. Lett.* **103**, 153002 (2009).
- ²⁶M. J. J. Vrakking and S. Stolte, *Chem. Phys. Lett.* **271**, 209 (1997).
- ²⁷T. Kanai and H. Sakai, *J. Chem. Phys.* **115**, 5492 (2001).
- ²⁸J. Wu and H.-P. Zeng, *Phys. Rev. A* **81**, 053401 (2010).
- ²⁹M. Machholm and N. E. Henriksen, *Phys. Rev. Lett.* **87**, 193001 (2001).
- ³⁰C. M. Dion, A. Keller, and O. Atabek, *Eur. Phys. J. D* **14**, 249 (2001).
- ³¹C.-C. Shu, K.-J. Yuan, W.-H. Hu, and S.-L. Cong, *Phys. Rev. A* **80**, 011401 (2009).
- ³²A. Sell, A. Leitenstorfer, and R. Huber, *Opt. Lett.* **33**, 2767 (2008).
- ³³M. Born and R. Oppenheimer, *Ann. Phys.* **389**, 457 (1927).
- ³⁴X.-L. Huang and X.-X. Yi, *Phys. Rev. A* **80**, 032108 (2009).
- ³⁵R. González-Férez and P. Schmelcher, *Phys. Rev. A* **71**, 033416 (2005).
- ³⁶R. González-Férez and P. Schmelcher, *New J. Phys.* **11**, 055013 (2009).
- ³⁷D. Sugny, A. Keller, O. Atabek, D. Daems, S. Guérin, and H. R. Jauslin, *Phys. Rev. A* **69**, 043407 (2004).
- ³⁸A. Matos-Abiague and J. Berakdar, *Phys. Rev. A* **68**, 063411 (2003).
- ³⁹I. S. Averbukh and R. Arvieu, *Phys. Rev. Lett.* **87**, 163601 (2001).
- ⁴⁰N. E. Henriksen, *Chem. Phys. Lett.* **312**, 196 (1999).
- ⁴¹C.-C. Shu, J. Yu, K.-J. Yuan, W.-H. Hu, J. Yang, and S.-L. Cong, *Phys. Rev. A* **79**, 023418 (2009).
- ⁴²H. Partridge and S. R. Langhoff, *J. Chem. Phys.* **74**, 2361 (1981).
- ⁴³P. F. Weck, K. Kirby, and P. C. Stancil, *J. Chem. Phys.* **120**, 4216 (2004).
- ⁴⁴H. Harde and D. Grischkowsky, *J. Opt. Soc. Am. B* **8**, 1642 (1991).
- ⁴⁵T. Seideman, *Phys. Rev. Lett.* **83**, 4971 (1999).
- ⁴⁶H. Stapelfeldt and T. Seideman, *Rev. Mod. Phys.* **75**, 543 (2003).
- ⁴⁷D. Daems, S. Guérin, D. Sugny, and H. R. Jauslin, *Phys. Rev. Lett.* **94**, 153003 (2005).
- ⁴⁸W. Yang, X. Song, S. Gong, Y. Cheng, and Z. Xu, *Phys. Rev. Lett.* **99**, 133602 (2007).
- ⁴⁹W. Yang, X. Song, C. Zhang, and Z. Xu, *J. Phys. B* **42**, 175601 (2009).
- ⁵⁰C.-C. Shu, K.-J. Yuan, W.-H. Hu, J. Yang, and S.-L. Cong, *Phys. Rev. A* **78**, 055401 (2008).
- ⁵¹W.-H. Hu, C.-C. Shu, Y.-C. Han, K.-J. Yuan, and S.-L. Cong, *Chem. Phys. Lett.* **474**, 222 (2009).
- ⁵²D. Sugny, A. Keller, O. Atabek, D. Daems, C. M. Dion, S. Guérin, and H. R. Jauslin, *Phys. Rev. A* **69**, 033402 (2004).
- ⁵³C.-Y. Wu, G.-P. Zeng, Y.-N. Gao, N. Xu, L.-Y. Peng, H.-B. Jiang, and Q.-H. Gong, *J. Chem. Phys.* **130**, 231102 (2009).
- ⁵⁴H. Hasegawa and Y. Ohshima, *Phys. Rev. Lett.* **101**, 053002 (2008).
- ⁵⁵A. S. Meijer, Y. Zhang, D. H. Parker, W. J. van der Zande, A. Gijsbertsen, and M. J. J. Vrakking, *Phys. Rev. A* **76**, 023411 (2007).
- ⁵⁶H. Hasegawa and Y. Ohshima, *Phys. Rev. A* **74**, 061401 (2006).
- ⁵⁷S. Bickman, P. Hamilton, Y. Jiang, and D. DeMille, *Phys. Rev. A* **80**, 023418 (2009).
- ⁵⁸I. Barth, L. Serrano-Andrés, and T. Seideman, *J. Chem. Phys.* **129**, 164303 (2008); **130**, 109901 (2009).
- ⁵⁹I. Barth, J. Manz, and L. Serrano-Andrés, *Chem. Phys.* **347**, 263 (2008).
- ⁶⁰Y.-H. Chen, S. Varma, A. York, and H. M. Milchberg, *Opt. Express* **15**, 11341 (2007).